

Comparison of the NDVI, ARVI and AFRI Vegetation Index, Along with Their Relations with the AOD Using SPOT 4 Vegetation Data

Gin-Rong Liu^{1,2}, Chih-Kang Liang², Tsung-Hua Kuo^{1,3}, Tang-Huang Lin¹, and Shih-Jen-Huang⁴

(Manuscript received 19 February 2003, in final form 28 October 2003)

ABSTRACT

For decades, the satellite images acquired in visible and infrared bands have been used for environmental monitoring. In this purpose, the normalized difference vegetation index (NDVI) is the commonly used vegetation index model for canopy monitoring and biomass assessment. However, due to the fact that the NDVI index is susceptible to various outside influences - most notably the atmospheric disturbance and currently more bands are provided by satellite platforms - additional indexes have been developed to counter these effects. This paper explores two such indexes - the Aerosol Free Vegetation Index (AFRI) and the Atmospherically Resistant Vegetation Index (ARVI). Comparisons were made with the NDVI index to see if they indeed performed better. The relationship of the different outcomes exhibited between the indexes with the aerosol optical depth (AOD) was analyzed and exploited to see if this scattering effect was more reduced than with NDVI. In general, the results showed that the AFRI and ARVI (with gamma = 1) indeed did perform better than their NDVI counterpart study with the related channels were employed.

(Key words: Vegetation index, NDVI, Aerosol optical depth)

1. INTRODUCTION

For decades, the normalized difference vegetation index (NDVI) is one of the most widely used indexes in assessing the amount of vegetation biomass (Rouse et al. 1973), especially for some commonly used resource satellites' images, such as Landsat TM and MSS, and SPOT

¹ Center for Space and Remote Sensing Research, National Central University, Chung-Li, Tawan, ROC

² Institute of Atmospheric Physics, National Central University, Chung-Li, Taiwan, ROC

³ Institute of Space Science, National Central University, Chung-Li, Taiwan, ROC

⁴ Department of Oceanography, National Taiwan Ocean University, Keelung, Taiwan, ROC

* *Corresponding author address:* Gin-Rong Liu, Center for Space and Remote Sensing Research, National Central University, Chung-Li, Tawan, ROC; E-mail:grliu@csrsr.ncu.edu.tw

satellite imagery. The NDVI index is mainly based upon the different behaviors exhibited by the vegetation toward different electromagnetic wavelengths: the chlorophyll inside the vegetation absorbs the energy situated within the red wavelength, while the mesophyll reflects back the infrared segment. Both the chlorophyll and mesophyll are essential elements in the photosynthesis process for plants. By tuning to these specific wavelengths, the sensors onboard satellites or aircrafts can measure the amount of reflectance from the surface, and calculate the value of the NDVI index by,

$$\text{NDVI} = (\rho_{\text{NIR}} - \rho_{\text{RED}}) / (\rho_{\text{NIR}} + \rho_{\text{RED}}), \quad (1)$$

where ρ_{NIR} refers to the near infrared reflectance and ρ_{RED} refers to the red band reflectance. The equation produces a value from -1 to +1, where each specific interval roughly represents a type of land canopy which mainly refers to the vegetation biomass ratio. Basically, when the index is below 0, it is the detection of clouds or snow; when it is between 0 and 0.1; it represents rocks, senescent vegetation or soil; when it is between 0.1 and 0.4, it is indicative of cities; when it is above 0.4, it implies the presence of vegetation biomass. The closer it is to the value of 1, the larger the amount of vegetation biomass there will be.

Because of the success of NDVI in plant surveying, other relevant parameters such as the leaf area index (LAI), vegetation fractional cover (French et al. 1997), chlorophyll concentration (Buschmann and Nagel 1993) and so forth can be derived to retrieve pertinent information from this index. Further, its relations with global CO_2 concentration have also been analyzed and studied (Tucker et al. 1986). The NDVI can be of great use in studying the remote sensing of vegetation physiology. Unfortunately, the scattering effects from the aerosols suspended in the atmosphere still can affect the reflectance observed by the space-borne sensors. Thus, several indexes have been formulated with similar vegetation index functions in hopes of eliminating or at least decreasing the influence induced by these atmospheric particles. The Aerosol Free Vegetation Index (AFRI) was conceived by simulating the reflectance of the red band with the short-wave infrared wavelength (SWIR) because of its capacity in penetrating through the atmospheric haze (Karnieli et al. 2001). The Atmospherically Resistant Vegetation Index (ARVI) uses a similar approach but by utilizing the blue band to conduct corrections on the red band (Kaufman and Tanre 1992). By using data from the newer generation Spot 4 VEGETATION sensor (Kaufman 1997), this study strives to compare the two indexes with the NDVI index by comparing them to the aerosol optical depth (AOD). Furthermore, the paper employs the ground truths of AODs to investigate the capacity of reducing atmospheric effect of these vegetation indexes.

2. THEORETICAL BASIC

2.1 ARVI Model

The main feature of the ARVI index is its capacity to reduce the influence from the atmosphere by employing the blue band in conducting atmospheric corrections on the red band. It's

a self-correcting process in image-based consideration (Kaufman and Tanre 1992). Compared to the red band, the blue band is much more easily scattered by the atmosphere particles. This explains why the sky is usually perceived as being blue. Thus, the ARVI index takes advantage of the different scattering responses from the blue and red band to retrieve information regarding the atmosphere opacity, and can be written as follows

$$\text{ARVI} = (\rho_{\text{NIR}} - \rho_{\text{rb}}) / (\rho_{\text{NIR}} + \rho_{\text{rb}}), \quad (2)$$

where ρ_{NIR} is the reflectance of the near infrared, ρ_{rb} equals $\rho_r - \gamma(\rho_b - \rho_r)$, γ (gamma value) is like a weighting function that depends on the aerosol type, and ρ_r and ρ_b refer to the reflectance of the red and blue bands, respectively.

The main reason why the blue band is more susceptible to atmospheric scattering than the red band is because its wavelength is shorter. Generally, the shorter wavelength has stronger scattering. It's very similar to the way sea waves behave over oceans. When a large wave strikes an object, such as a ferryboat, it is more capable of continuing on its path by going around the object. On the other hand, it is dispersed more easily when the waves are smaller in size. Consequently, by obtaining the difference between the reflectance of the highly sensitive blue band and the less sensitive red band ($\rho_b - \rho_r$), it serves like an indicator of what the atmospheric conditions were like. Here γ serves as a weighting function for the difference reflectance of the two bands. Various values can be chosen for γ , which mainly depends on the type of aerosol size, but according to Kaufman and Tanre's statement in 1992, it is best to select a gamma value of 1 "when information on the aerosol type is not available". Consequently, the main purpose of $\rho_r - \gamma(\rho_b - \rho_r)$ is to decrease the influence brought forth from the atmosphere, where a more accurate assessment of the value of the red reflectance can be obtained. The index again yields a similar scale ranging between -1 and 1.

2.2 AFRI Model

AFRI uses primarily the short-wave infrared wavelength (SWIR) in developing its vegetation index. The SWIR has both the advantage of being sensitive to vegetation while at the same time being less susceptible to the influence of aerosols. This is mainly because its wavelength is considered much larger than the radius of most aerosols, except for the very large dust particles, which allows it to be more capable of circumventing the suspended particles. Thus, the AFRI index makes use of this aspect by seeking to replace, or in another sense, simulate the reflectance of the red band with the SWIR wavelength. This is done by first finding the mathematical relationship between the two bands under clear-sky conditions. With the devised equation, the value of the actual red reflectance can be better calculated with the SWIR under the influence of aerosols. Even if there were no aerosols present, the index could still "be a match for the NDVI index" (Karnieli et al. 2001). Its correlation with the NDVI index may reach 0.98 for various land cover types, which is certainly extremely high. The AFRI is written as follows,

$$\text{AFRI}_{2.1} = (\rho_{\text{NIR}} - 0.5\rho_{2.1}) / (\rho_{\text{NIR}} + 0.5\rho_{2.1}), \quad (3)$$

$$\text{AFRI}_{1.6} = (\rho_{\text{NIR}} - 0.66\rho_{1.6}) / (\rho_{\text{NIR}} + 0.66\rho_{1.6}), \quad (4)$$

where the subscripts 2.1 and 1.6 refer to the reflectance of different wavelengths in μm situated within the SWIR region, and ρ_{NIR} denotes the reflectance of the near infrared. Both the 2.1 and 1.6 μm wavelengths can be chosen because they are situated within atmospheric windows, where they are less affected by absorbing atmospheric gases. The index produces a dynamical range similar to that of the NDVI and AVRI, ranging between -1 and +1. However, due to the fact that the Spot 4 VEGETATION data used in this paper contain reflectance data only from the 1.6 μm wavelength, only the second equation of the AFRI index can be tested.

3. DATA

Some earlier resource satellites mainly provided observations in visible and near and thermal infrared regions. With the improvements in the data acquisition techniques, modern satellites, especially for hyperspectrum sensors, provide more and narrower bands than ever. With this advantage, more accurate band combinations could be employed. For example, the data used in this study were acquired from the Spot 4 VEGETATION instrument (VI) sensor. The Spot 4 satellite, one of the newest additions in the series of Spot satellites, was lifted into a sun-synchronous orbit onboard an Arian 4 launch vehicle on March 24, 1998 and is operated by Spot Imaging of France. The VI sensor's primary mission is in the environmental monitoring of the Earth's surface. Its total field of view is 50.5° , where it has a swath width of 2250 km. The spatial resolution is 1 km across the entire field of view (FOV). The VI sensor provides data in four separate channels - 1) Blue: 0.43~0.47 μm , 2) Red: 0.61~0.68 μm , 3) Near infrared: 0.78~0.89 μm , 4) SWIR: 1.58~1.75 μm . The satellite scans the Earth through linear array detectors, and orbits the planet 14 times a day, where its equatorial crossing time is 10:30 a.m. The Spot 4 data used in this study were acquired by the Center for Space and Remote Sensing Research (CSRSR) at the National Central University (NCU) in Taiwan.

4. VEGETATION ANALYSIS

4-1. Vegetation Index Comparison

An image set of vegetation index maps derived by various model are showed in Fig. 1. The results showed that the subtle differences around some areas could be distinguished, especially for the coastal zones around the southeastern Mainland and the East Sea. In addition, a typhoon pattern was shown in various contrast patterns around the lower corner. It is obvious that the different information could be enhanced with different vegetation indexes. For further analysis, three months of data from September 14 to November 26 of the year 2001 were mainly processed in constructing the various vegetation index images. Initially, the target area was confined to eastern Asia, including Taiwan. Because there were too many cloudy days

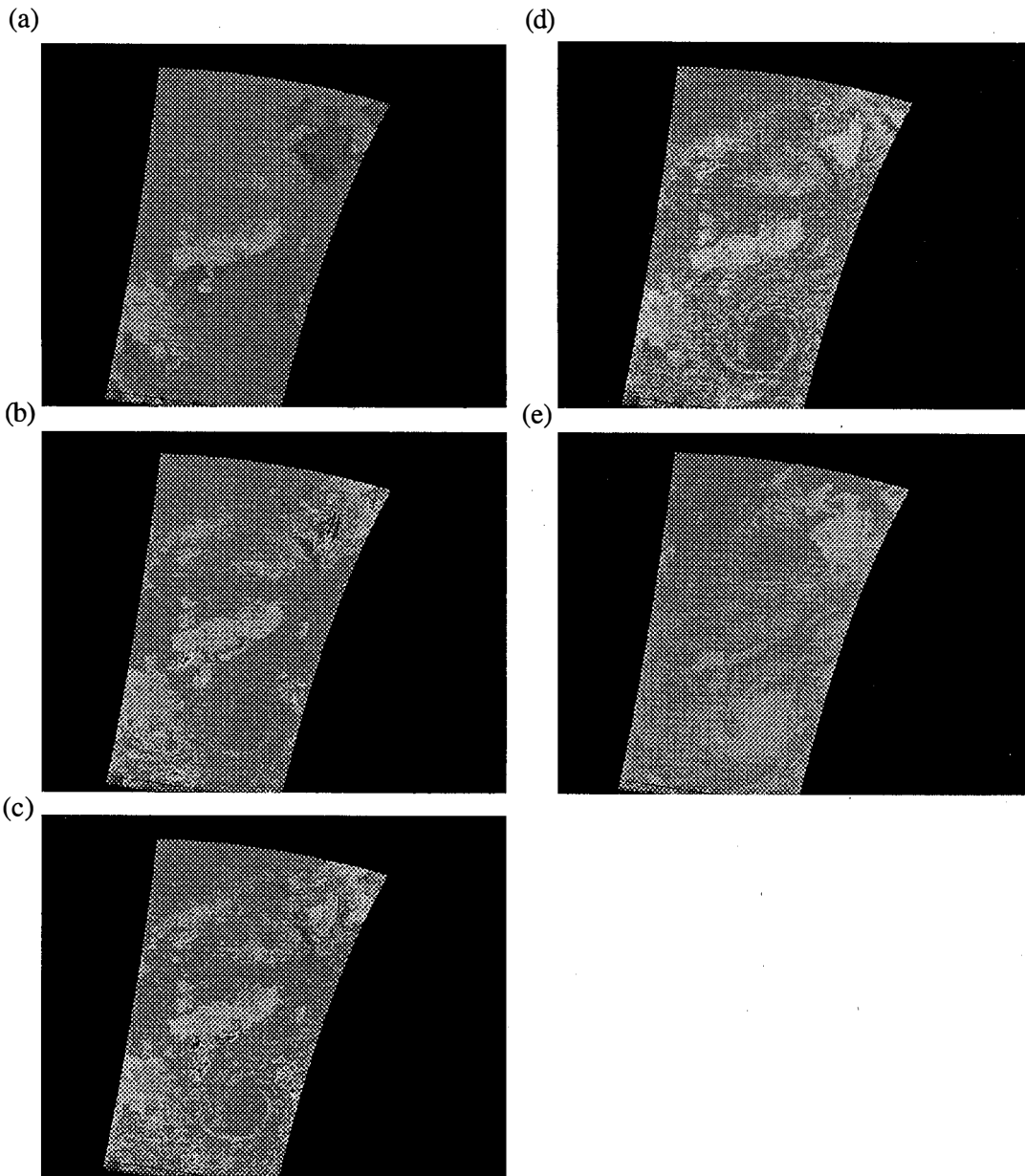


Fig. 1 Grayscale image of the (a)NDVI, (b)ARVI ($\gamma = 0.7$), (c) ARVI ($\gamma = 1.0$), (d) ARVI ($\gamma = 1.3$), (e) AFRI index during 2001/11/10.

during this period, we ended up having roughly 20 sets or so of images with much cloud-free area for the analysis in this study. A large portion of the images selected occurred during November, which on a yearly average, contains the least amount of cloud cover over Taiwan.

A set of total 80 points (locations) where were cloud-free were chosen randomly from the 20 sets images and computed their different vegetation indexes in comparing the ARVI and AFRI indexes with the NDVI (Fig. 2). The points were chosen throughout the image, including the island of Taiwan. The digital counts selected were subsequently recalculated into their

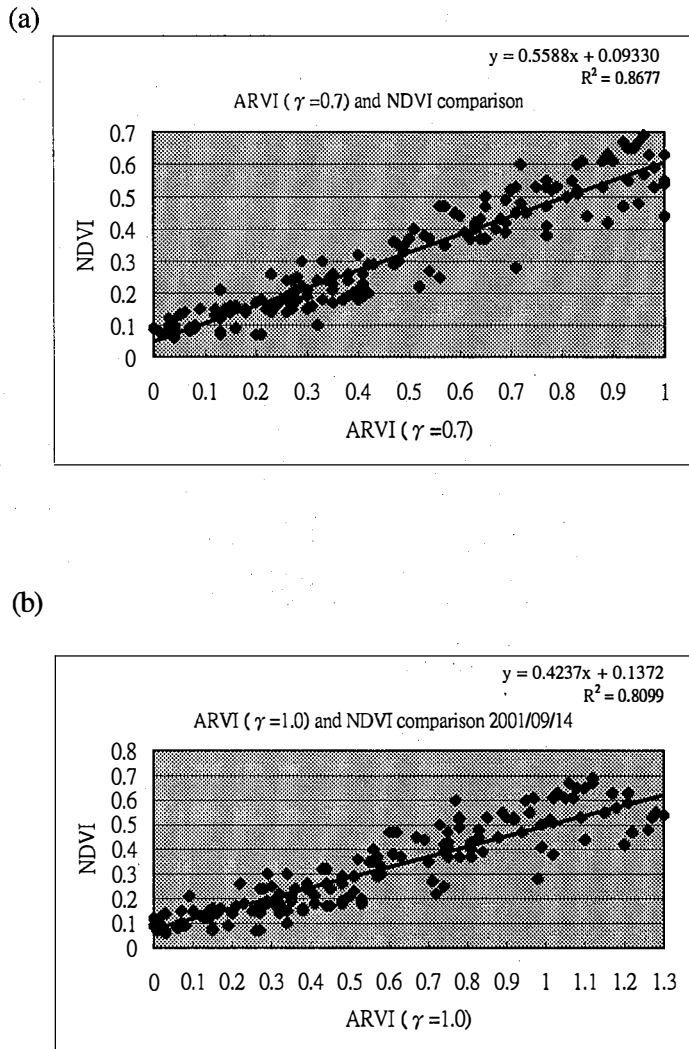
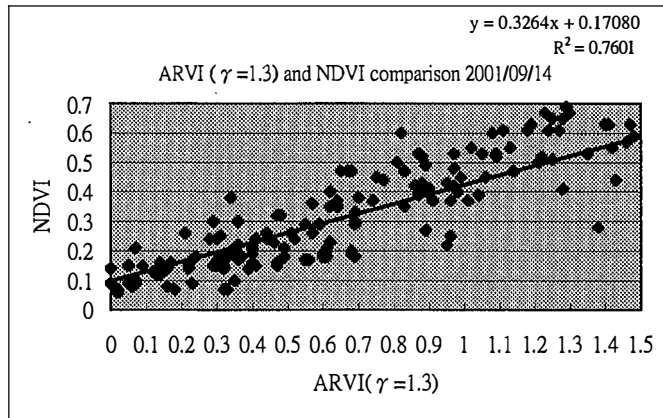
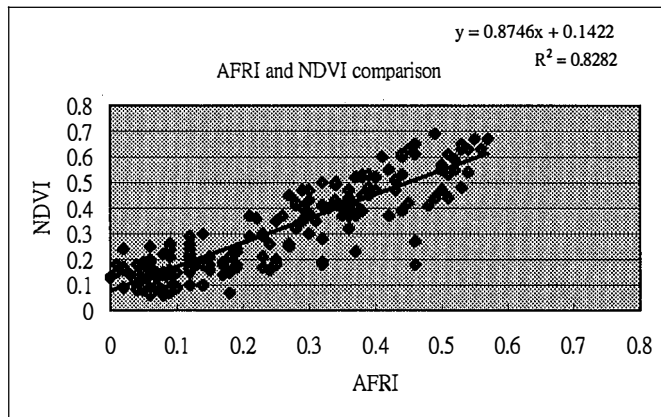


Fig. 2 (a) Comparison of the ARVI ($\gamma=0.7$) and NDVI index, (b) but for $\gamma=1.0$, (c) but for $\gamma=1.3$, (d) but for AFRI, (e) but for the ARVI ($\gamma=1.0$) and AFRI.

(c)



(d)



(e)

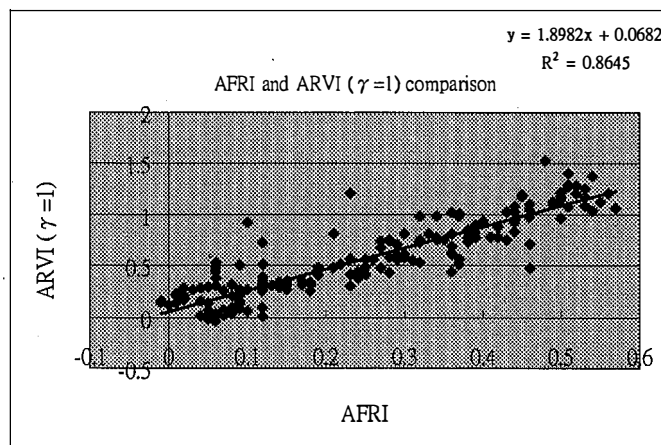


Fig. 2 (continued)

respective index values. Theoretically, when the correlation is higher, it indicates that the AOD is lower, allowing the vegetation indexes to behave more similarly. On the other hand, if the correlation is lower, it should indicate that the NDVI has been affected by a higher AOD over certain places. In general, the r^2 of the ARVI and AFRI models all reached to 0.8 except the ARVI (= 0.76 with $\gamma=1.3$), meaning the ARVI and AFRI both provide indications similar to those the NDVI provided. Of course, some subtle differences could be caught.

By first looking at the AFRI index, the average r^2 is roughly around 0.7 to 0.8. Based upon some single days' computations in November, it was found that a lower correlation was observed, suggesting the aerosol content may have been higher over some locations, thus causing the NDVI index values to drop. If so, this may be evidence that the AFRI index is indeed more capable of deterring the atmospheric influence. In addition to calculating the vegetation biomass over the land, an unexpected surprise was found when processing the AFRI index images. Various bright areas, especially around the coastal zones, could also be spotted over oceans (Fig. 3). By comparing them with images from the ocean monitoring satellite SeaWiFS (see also Fig. 3, upper panel), quite a nice correspondence appeared to exist. This layout can be seen, once again from Fig. 3, where the bright areas indicated by green arrows (the lower left panel) of the AFRI image matches quite well with the chlorophyll distribution image from SeaWiFS. In contrast, the NDVI image is completely incapable of doing so, as the digital counts registered are very low over oceans. However, the similarity was not attributed to the existence of chlorophyll concentration, but was correlated with the existence of river sediment over the coastal zone because the value of ρ (near IR) is much closer to zero over open ocean than its value over coastal zone where river sediment concentration is high. In addition, the concentration of suspended particles in the coastal zone may be a few orders higher than the chlorophyll concentration. However, the distribution pattern is rather close to the pattern of the chlorophyll concentration derived from SeaWiFS imagery. The relation between river sediment and chlorophyll and the accuracy of the chlorophyll derivation (especially in SeaWiFS) is worthy of further study. This interesting discovery may be further explored by expanding the potential of the AFRI index into the monitoring of the suspended particles over coastal zone.

Turning our attention to the ARVI index, the gamma values of 1, 1.3 and 0.7 were tested respectively to see how it correlated with the NDVI index. The reason for adding 0.7 and 1.3 was to analyze how they performed differently from the usual assumption of $\gamma=1$. Borde et al. 2003 stated that a value of 1.3 was instead deemed more suitable over their research area located in France. Based on this account, it may be possible that a different gamma value could be more appropriate for the Asian area. However, after checking the pixels throughout the area, we found that our comparison disproved the possibility and indicated that the $\gamma=1.0$ provided a better result. Another probable reason is from the influence of cirrus clouds located in the upper atmosphere that are hard to detect.

As for when gamma equals 1.3, the lower r^2 also occurred during November. Furthermore, the overall correlation for each date was lower. The reason for the sudden drop may be attributed to the fact that the weighting factor of 1.3 was too high, rendering the values of the ARVI index to go up too much, or put in another way, producing a possible "over-correction". Quite the opposite was observed between the NDVI and ARVI index when $\gamma=0.7$. The relationship

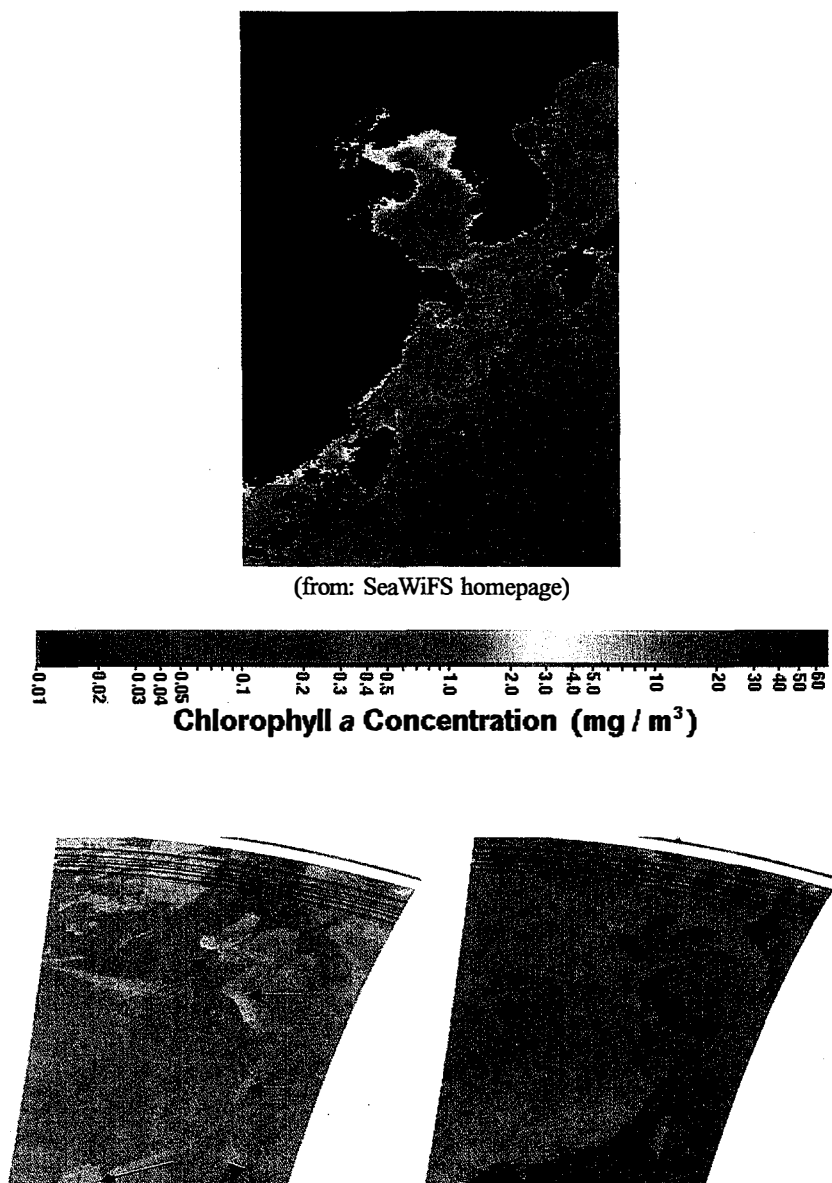


Fig. 3 The left image represents the AFRI index acquired during 11/26/2001. Arrows indicate bright areas with high concentrations of chlorophyll that correspond to the SeaWiFS image above. The right image represents the NDVI. The red dot in the upper panel is the location of the Anmyon Aeronet Station.

between the two exhibited a strong correlation for each date, where the lowest r^2 still retained a value of 0.82. Although the lower correlation values observed corresponded to the dates when $\gamma = 1$ and 1.3, the values were still exceptionally high. The relationship between the two was unreasonably too close, or put in another way, the two behaved too similarly with each other. The reason for this phenomenon may be due to the fact that the gamma value was too low, causing a so-called "under-correction". Consequently, when gamma equaled 0.7, it seemed it was unable to carry out its designed purpose of filtering enough away the influence from atmospheric aerosols. The distance toward the regression line for most of the points was quite short, producing the wrong impression that the AOD were all very low during those dates. Therefore, it would appear that a gamma value centered roughly at 1.0 would be regarded as a more suitable assumption.

4-2. AOD Analysis

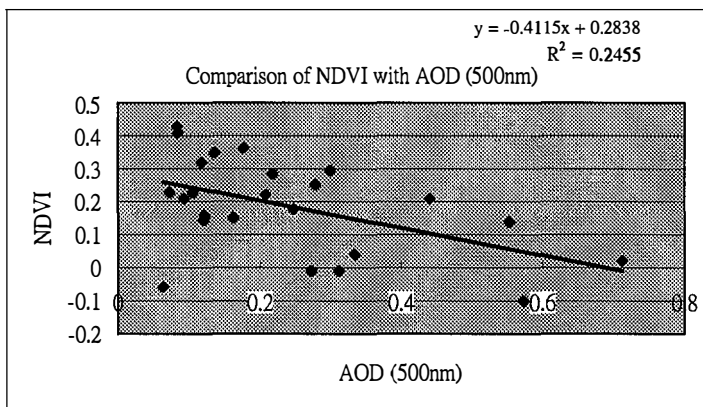
The primary influence the atmosphere exerts on the vegetation index arises from the aerosols it contains, which is measured quantitatively by the aerosol optical depth. According to the glossary from the book entitled, *The Remote Sensing Data Book*, aerosols are "a suspension of very small (typically 1 nm to 10 μm) solid particles (e.g., dust, sulphates) or liquid droplets in air, mostly found in the atmospheric boundary layer". Aerosols can originate naturally, like from the recent dust storm events detected over Mongolia, or they can be manmade, such as from industrial pollution or biomass burning. These suspended particles play a very important role in remote sensing because of their capacity to scatter radiation.

Originally, some dates of images that were used to compare the vegetation indexes were intended to be selected in comparing the AOD analysis by utilizing several stations from the Aerosol Robotic Network (Aeronet) that were near the thirty points previously chosen from the vegetation index image for each date when the Aeronet observations were available. Aeronet is a vast network comprised of stations scattered across the world that are used in the monitoring of the aerosol optical depth with ground-based instruments. At first, roughly around four to five stations were deemed suitable sites, but due to the data available from each station, finding areas where they were cloud-free and the requirement of the image acquisition time from the Vegetation sensor to coincide or at least be near the time of the AOD measurement (within 20 minutes), the AOD analysis was conducted primarily from the Anmyon station of South Korea only. The station is situated at a latitude of 36.5° and a longitude of 126.3° , where it is located on an islet west of South Korea (see also Fig. 3). A total of twenty-four dates were selected from the three-month long period from the station based once again on the three factors mentioned above. Four types of AOD data were selected, with wavelengths situated in the green (500 nm), blue (440 nm) red (670 nm) and near infrared (870 nm). In addition to the images constructed in illustrating the three vegetation indexes, images depicting the respective reflectance of the four spectral channels were also processed (Figs. 4, 5, 6, 7 and 8). Due to the fact that the longitude and latitude grid had not been yet been constructed, the exact location of the station from the processed Spot image data could not be determined. Thus, a 3 x 3 window was chosen near the area where the values of the nine pixels from the window

were subsequently averaged to approximate the value of the respective vegetation index or reflectance near the vicinity of the station. Scatter plots of each respective vegetation index with the AOD were then drawn for analysis.

From the slope of Fig. 4a, we see that the NDVI index value goes down steeply with an increasing AOD. This is consistent with the fact that a higher AOD causes the suspended particles in the atmosphere to scatter the red band more. This increased scattering may produce a larger reflectance in the red band than NIR for the sensor to detect, and thus render the value of the NDVI index to drop. As for the scatter plot of the AFRI index with the AOD (Fig. 4e), the regression line slopes a little upward with an increasing AOD. This indicates that the

(a)



(b)

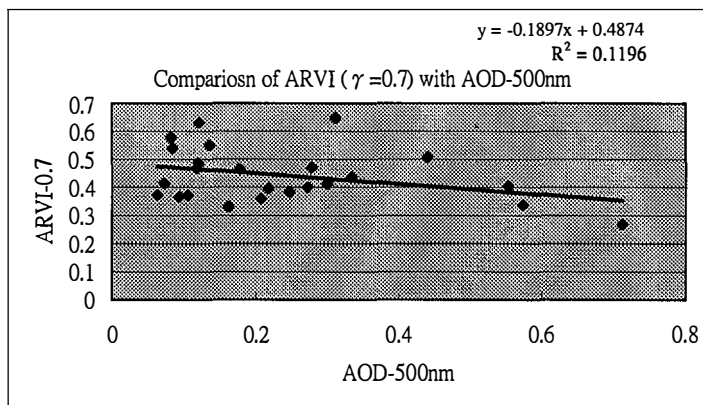
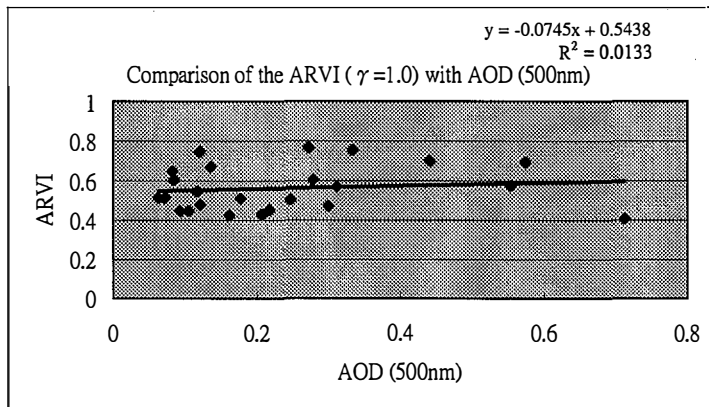
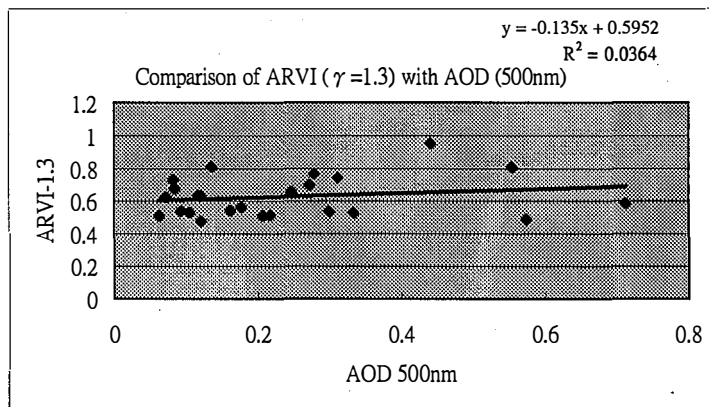


Fig. 4 (a) Comparison of the NDVI index and AOD - 500 nm, (b) but for ARVI ($\gamma=0.7$), (c) but for ARVI ($\gamma=1.0$), (d) but for ARVI ($\gamma=1.3$), (e) but for AFRI.

(c)



(d)



(e)

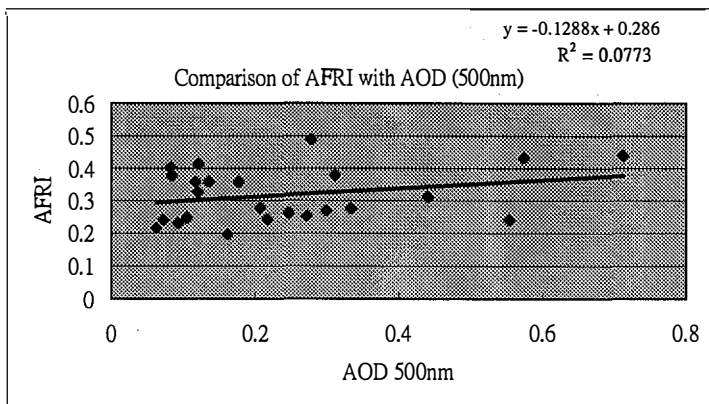


Fig. 4 (continued)

SWIR can still be slightly affected from an increasing AOD, but not as much as the red band. Finally, for the ARVI index (Figs. 4b,c,d), when gamma equals 1.3, the regression lines tilts up a little; when gamma equals 1, it becomes nearly horizontal; and when gamma equals 0.7, it slightly edges down. The more horizontal the regression line is, the more likely it is not so easily affected by the AOD. Here, the lower correlation coefficients indicate that that model is less sensitive to the AOD variation. In other words, the models, which have lowest correlation relation is what we want. Therefore, it seems logical to assume that the AFRI index and the ARVI index with a gamma value of 1.0 would be the most capable of overcoming the influence of aerosols.

Scatter plots of the AOD plotted against the reflectance of the near infrared, red, blue, and SWIR reflectance were also drawn for analysis. From Fig. 5, the reflectance of the near infrared decreases a little as the value of the AOD increases. This may be attributed to the fact that the suspended particles in the atmosphere absorb a certain amount of the near infrared radiation. The same trend can also be observed for the SWIR reflectance with the AOD, except that the regression line is not as steep, implying that the absorption may not be as strong, which explains why the AFRI index takes advantage of this band (Fig. 6). However, the graphs of the red and blue band wavelengths versus their respective AOD show quite the opposite (Fig. 7 and 8). A larger AOD brings forth also a larger reflectance value. This is consistent with the fact that the scattering effect is much stronger in these bands especially for the blue band, which is why the ARVI index uses it to correct the red band. Based upon the previous discussions, we found that the NDVI is more easily affected by the AOD than the AFRI or ARVI vegetation indexes. Surely, the differences are mainly related to the values of AOD. So, it was conjectured that the difference with the AFRI or ARVI values could be used in indirectly investigating the AOD variation or subtle information over a certain location. In other words, use the AFRI and ARVI to serve as a baseline in making the subtraction. This could be

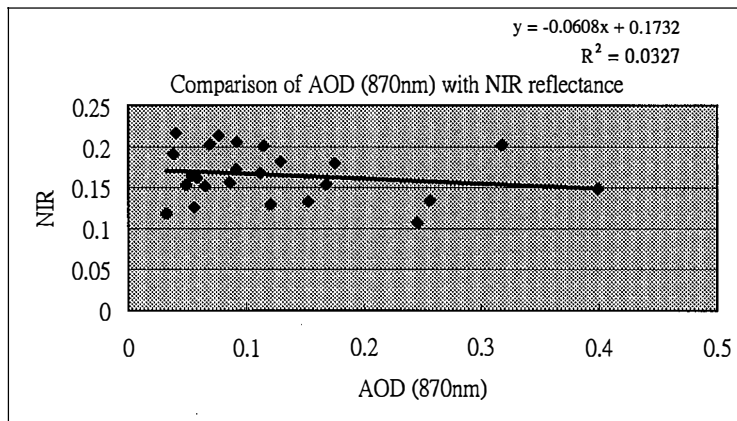


Fig. 5 Comparison of the Near infrared reflectance and AOD - 870 nm.

done if a linear equation can be derived between the AOD and vegetation index difference. However, the conjecture requires more data and studies to figure out the possible algorithm and applications.

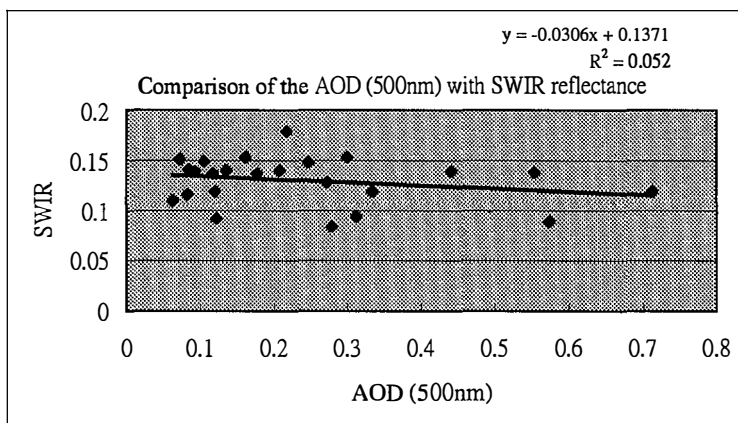


Fig. 6 Comparison of the SWIR reflectance and AOD - 500 nm.

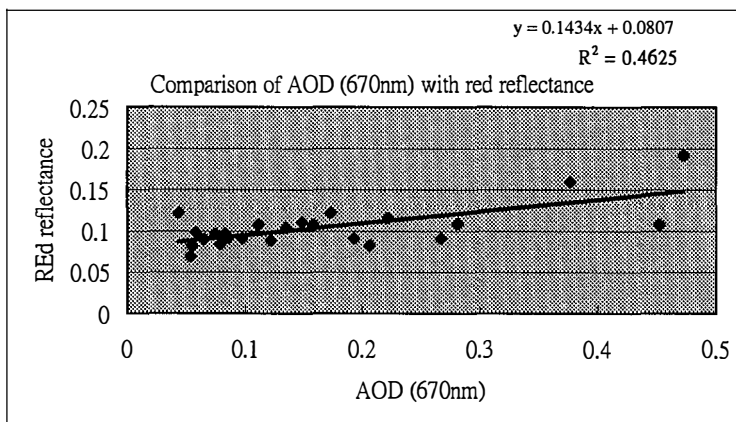


Fig. 7 Comparison of the Red reflectance and AOD - 670 nm.

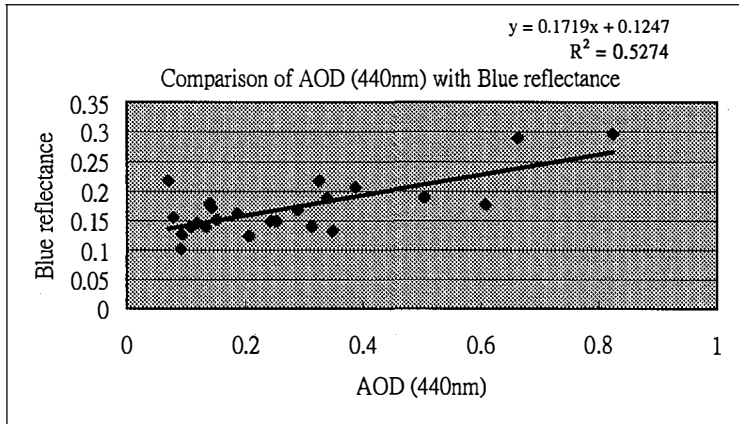


Fig. 8 Comparison of the Blue reflectance and AOD - 440 nm.

5. CONCLUSIONS

Through comparisons of the three vegetation indexes, it appears that the AFRI and ARVI index with $\gamma = 1$, seem to be the most capable in reducing the atmosphere effects. In contrast, an over-correction appears to occur when $\gamma = 1.3$, and an under-correction seems to occur when $\gamma = 0.7$ value. In addition, the value of 0.7 demonstrated the lowest fluctuation throughout the changes in the AOD. This contradicts the fact that the gamma value of one supposedly is the most capable of decreasing the atmospheric influence. Consequently, more research should be done regarding the value of 0.7. Furthermore, it is also suggested that additional gamma values different from 0.7 and 1.3 should be tested in the future. Perhaps it is still possible that a different gamma value exists for the Asian area. It is possible that the vegetation indexes are affected by other important parameters other than the AOD. Therefore, although the aerosol optical depth is a crucial factor affecting the index value, other relevant factors that seemingly cannot be ignored, should be further looked into. Also, more analyses should also be done regarding why the range of the ARVI index values was larger than expected. Moreover, perhaps through the expanded range, it could be used in making even more precise land cover classifications. It is also suggested in testing the $2.1 \mu\text{m}$ channel for the AFRI index with other sensor data, because theoretically, it is even more capable of penetrating through the atmospheric haze as the wavelength is even longer.

Finally it is still premature to make any conclusions regarding whether the differences of different AOD can be employed to retrieve other aerosol information. As there were only twenty-four sets of data to test our procedure, more data must be processed and analyzed. In addition, one of the main inaccuracies might be attributed by scattered cirrus clouds in the

atmosphere that are not easily detected. More efforts to provide reliable cirrus cloud screening are strongly encouraged. On the other hand, the theoretical basis of the ARVI index is complex and not as direct as AFRI. It's probable that eventually the AFRI index will attain a more important role in future studies. Its physical interpretations are clear and more direct. When devising an index, it must be both simple and resistant to various influences. In addition, its potential in assessing the chlorophyll over the ocean and in calculating the AOD with the NDVI index should be further explored. Perhaps a whole new index could be devised with the new method. Lastly, with the recent launch of the SPOT 5 spacecraft in 2002, which carried onboard the second-generation VEGETATION instrument, more precise measurements can be made of our home planet's surface. As the spectral resolution of satellites continues to improve, and new innovative ways are being invented to remotely sense our planet, there is still much more to be learned of our beautiful planet.

Acknowledgments Authors are very grateful to Mr. Long-Sin Liang and Mr. Jen-Yen Fan for their help in data processing. The research was supported by the Council of Agriculture, Taiwan under grant 91AS-5.1.1-FC-R2.

REFERENCES

- Ahrens, C. D., 1994: *Meteorology Today An Introduction to Weather, Climate, and the Environment*, 5th Ed. West Publishing Company, 591pp.
- Borde, R., D. Ramon, C. Schmechtig, and R. Santer, 2003: Extension of the DDV concept to retrieve aerosol properties over land from the Modular Optoelectronic Scanner sensor. *International Journal of Remote Sensing*, **24**, 1439-1467.
- Buschmann, C. and E. Nagel, 1993: In vivo spectroscopy and internal optics of leaves as basis for remote sensing of vegetation. *International Journal of Remote Sensing*, **17**, 845-862.
- Carlson, T. N. and D. A. Ripley, 1997: On the Relation between NDVI, Fractional Vegetation Cover, and Leaf Area Index. *Remote Sensing Environ.*, **62**, 241-252.
- Fedosejevs, G., N. T. O'Neill, A. Royer, P. M. Teillet, A. I. Bokoye, and B. McArthur, 2000: Aerosol Optical Depth for Atmospheric Correction of AVHRR Composite Data (printed from the Internet at <http://www.ccrs.nrcan.gc.ca/ccrs/>).
- Frank M. Jr., 2002: Mar4: Orbiting Gravity Mappers Might Spot Oil Fields. *Aviation Week and Space Technology*, 56-58.
- French, A. N., T. J. Schmugge, and W. P. Kustas, 2000: Discrimination of Senescent Vegetation Using Thermal Emissivity Contrast. *Remote Sensing Environ.*, **74**, 249~254.
- Karnieli, A., Y. J. Kaufman, L. Remer, and A. Wald, 2001: AFRI - Aerosol Free Vegetation Index. *Remote Sensing Environ.*, **77**, 10-21.
- Kaufman, Y. J. and D. Tanre, 1992: Atmospherically Resistant Vegetation Index (ARVI) for EOS-MODIS. *IEEE Trans. Geosci. Remote Sensing*, **30** (2), 261-270.

- Kaufman, Y. J., A. E. Wald, L. A. Remer, B. C. Gao, R. R. Li, and L. Flynn, 1997: The MODIS 2.1 μm Channel - Correlation with Visible Reflectance for Use in Remote Sensing of Aerosol. *IEEE Trans. Geosci. Remote Sensing*, **35**, 1286~1298.
- Kaufman, Y. J. and L. Remer, 1994: Detection of Forests Using Mid-IR Reflectance: An Application for Aerosol Studies. *IEEE Trans. Geosci. Remote Sensing*, **32**, 672-683.
- Liu, G. R., A. J. Chen, T. H. Lin, and T. H. Kuo, 2002: Applying Spot data to estimate the aerosol optical depth and air quality. *Environ Modelling & Software*, **17**, 3-9.
- Rees, G., 1999: The Remote Sensing Data Book. Cambridge University Press, 262pp.
- Rouse, J. W., R. H. Haas, J. A. Schell, and D. W. Deering, 1973: Monitoring vegetation systems in the great plains with ERTS. Third ERTS Symposium, Goddard Space Flight Center, Washington, DC. NASA SP-351, 390-317.
- Santer, R., V. Carrere, Ph. Dubuisson and J. C. Roger, 1999: Atmospheric corrections over land for MERIS. *International Journal of Remote Sensing*, **20**, 1819-1840.
- Tucker, C. J., I. Y. Fung, C. D. Keeling, and R. H. Gammon, 1986: Relationship between atmospheric CO₂ variations and a satellite-derived vegetation index. *Nature*, **319**, 195-198.
- Vane, G., A. Goetz., and F. H. Alexander, 1993: Terrestrial Imaging Spectrometry: Current Status, Future Trends. *Remote Sensing Environ.*, **44**, 117-226.